PERGAMON Journal of the Franklin Institute 338 (2001) 405–427

Journal *of* The Franklin Institute

www.elsevier.nl/locate/jfranklin

System fusion in passive sensing using a modified hopfield network

Yu.V. Shkvarko*, Yu.S. Shmaliy, R. Jaime-Rivas, M. Torres-Cisneros

Faculty of Mechanical, Electrical and Electronic Engineering, University of Guanajuato, Salamanca, C.P. 36730, Mexico

Received 3 February 2000; received in revised form 28 October 2000

Abstract

We address a new approach to the problem of improving the quality of remote-sensing images obtained with several passive systems, in which case we propose to exploit the idea of neural-network-based imaging system fusion. The fusion problem is stated and treated as an aggregate inverse problem of restoration of the original image from the degraded data provided by several image-formation systems. The non-parametric maximum entropy regularization methodology is applied to solve the restoration problem with the control of balance between the gained spatial resolution and noise suppression in the resulting image. The restoration and fusion are performed by minimizing the energy function of the multistate Hopfield-type neural network, which integrates the model parameters of all sensor systems incorporating a priori and measurement information. Simulation examples are presented to illustrate the good overall performance of the fused restoration achieved with the proposed neural network algorithm. © 2001 The Franklin Institute. Published by Elsevier Science Ltd. All rights reserved.

Keywords: Passive sensing; Maximum entropy; Image restoration; System fusion; Neural network

1. Introduction

The need for improving the quality of images arises in many practical applications, one of those is remote sensing imagery with several passive systems. Any remote-sensed image, which is actually formed, inevitably suffers from degradations due to

*Corresponding author. Fax: +52-464-72-400.

E-mail address: shkvarko@salamanca.ugto.mx (Yu.V. Shkvarko).

0016-0032/01/$20.00 © 2001 The Franklin Institute. Published by Elsevier Science Ltd. All rights reserved.
PII: S0016-0032(00)00084-3

the finite system resolution and noise in observations. The image restoration is an important problem in the theory and application of remote sensing, signal and image processing. It has received a great deal of attention in the past decades and many different techniques are now available, e.g. [1–26]. These methods can be roughly categorized into two classes: those, which work on the parametrical model-based properties of the images, and those that do not use image representation in a parametrical form. In this study, we will refer to the latter as restoration methods, since they are more suitable for real-world remote sensing scenarios because environmental scenes are usually too complex to be approximated by the finite-order parametrical models [4,14,18]. The maximum entropy (ME) approach [2,6,10,12,17] seems to be one of the most attractive among the non-parametrical image reconstruction methods. It has been successfully used in different application areas for the restoration of fine image structures severely degraded in a noisy environment. However, the greatest advantage of the ME method in spite of its seeming computational complexity is that it may be efficiently implemented using artificial neural network (NN) computing. Several Hopfield-type networks for digital image restoration were designed in [12,15,17,19,22] based on the basic regularization methodology for minimizing the energy function of the NN associated with the cost function of the corresponding optimization problem.

Increasing capability of co-registered multisystem remote sensing imagery has spurred development of various techniques for system data fusion. These techniques aim to produce the restored images with improved performances of information content, resolution and accuracy [7,9,13]. In engineering practice, it is very important, on one hand, to have some theoretical guarantees that the developed fusion method can improve the image performances before its application to real systems, but on the other hand, a unified computational structure of the fusion algorithm is desired, in which case it allows coping with different system models. For this reason, the framework of NNs is very convenient for fusion design because of the NNs' fault-tolerant nature, computational capabilities and flexible adjustment.

In this paper, the problem of image restoration with system fusion is stated and treated as an ill-conditioned inverse problem of restoration of the original image from the degraded images received from different passive-sensing systems. This problem is approached by exploitation of information on the performances of the corresponding systems combined with prior realistic knowledge about the properties of the scene contained in the ME a priori image model. A specific aggregate regularization problem is stated and solved to reach the aims of system fusion with control of the design parameters, which influence the overall restoration performances. To accomplish the system fusion computationally, we investigated the fine structure of the multistate maximum entropy neural network (MENN) proposed by Li et al. [22], and modified the MENN's algorithm to enable the network to solve the aggregate fusion and restoration problems. This was accomplished by processing the data provided by several imaging systems incorporating measurements, system calibration and image model information. We also present a quantitative and qualitative characterization of the performance of the developed MENN algorithm evaluated through software simulation, along with it

comparison with the regularized inverse filtering and NN-based image restoration and fusion techniques in an example of application to passive radar sensing.

The paper is organized as follows: Section 2 states the system fusion concept for image restoration. The regularization formalism of the problem is developed in Section 3. The MENN for system fusion is presented in Section 4 followed by simulation results in Section 5 and concluding remarks in Section 6.

2. The problem of image restoration with system fusion

2.1. Problem formulation

In passive sensing, the signal field, in which the system sensor or array of sensors are immersed, is assumed to be created by some continuous distribution of far-distant energy sources, each sending out traveling waves which sweep across the sensor array (antenna) as plane wave fronts. The various elementary sources are considered to be random and independent of one another. The spatial distribution of the average power of the signal wavefield impinging on the sensor system from different angular directions $\boldsymbol{\theta} \in \Theta \subset R^2$, is characterized by the spatial power spectrum pattern $v(\boldsymbol{\theta})$, which is referred to as the original image of the environment [1,2]. In remote sensing imagery [6,14], a model, which is most often used, expresses the degraded image produced by a passive system as a sum of the noise and a linear convolution of the original image with the system's antenna receiving pattern. The latter is usually referred to (in the terms of image processing theory [11,15]) as the point-spread function (PSF) of the image formation system. The noise is accounted to that of the system noise, components in the degraded image that correspond to environmental noise, and additive noise induced at the image recording stage. These noise components are usually modeled as statistically independent of the image and one another, while in some imaging scenarios the signal-dependent noise model may also be utilized [5,22]. Applying the linear model conventional for the practical remote sensing systems [6,14], the actual continuous image formed by the passive system is expressed as

$$u(\boldsymbol{\theta}) = \int_{\Theta} F(\boldsymbol{\theta}, \boldsymbol{\theta}') v(\boldsymbol{\theta}') \, \mathrm{d}\boldsymbol{\theta}' + n(\boldsymbol{\theta}), \quad \boldsymbol{\theta}, \boldsymbol{\theta}' \in \Theta, \tag{1}$$

where $F(\boldsymbol{\theta}, \boldsymbol{\theta}')$ is the system's PSF, which, in general, can be spatially varying, $v(\boldsymbol{\theta})$ the original image, $n(\boldsymbol{\theta})$ the noise in the image, and $u(\boldsymbol{\theta})$ the degraded image produced by the system.

Dependent on the assumed dimension of the environmental scene, one-dimensional ($\Theta \subset R^1$) or two-dimensional ($\Theta \subset R^2$) continuous images are considered in remote-sensing imagery [5,6,14,18]. To represent the digital-form approximation of the physical image formation model (1) define K-dimensional ($K-$D in our notation) image subspace $V_K(\Theta) = \mathrm{span}_{k \in K}\{\varphi_k(\boldsymbol{\theta})\}$ spanned by some chosen set of basis functions $\varphi_k(\boldsymbol{\theta})$ ordered by the index, $k = 1, \ldots, K$, which are considered to be real-valued orthonormal functions in $L^2(\Theta)$ Hilbert space [9]. The

orthogonal projections of the images $v(\boldsymbol{\theta})$, $u(\boldsymbol{\theta})$ and noise $n(\boldsymbol{\theta})$ onto $V_K(\Theta)$ are represented by the relevant vectors $\mathbf{v}$, $\mathbf{u}$ and $\mathbf{n}$ of their discrete-form approximations with the elements given by

$$v_k = [v(\boldsymbol{\theta}), \varphi_k(\boldsymbol{\theta})], \quad u_k = [u(\boldsymbol{\theta}), \varphi_k(\boldsymbol{\theta})], \quad n_k = [n(\boldsymbol{\theta}), \varphi_k(\boldsymbol{\theta})], \quad k = 1, \ldots, K, \tag{2}$$

where $[f, \varphi_k]$ defines the inner product of the corresponding real-valued functions in $L^2(\Theta)$ space, i.e. $[f, \varphi_k] = \int_\Theta f(\boldsymbol{\theta})\varphi_k(\boldsymbol{\theta})\, \mathrm{d}\boldsymbol{\theta}$. The $K-$D matrix-form approximation of the system's PSF $F(\boldsymbol{\theta}, \boldsymbol{\theta}')$ is given by the $K\times K$ non-negative "blur matrix" $\mathbf{F}$ with elements

$$F_{ki} = [F(\boldsymbol{\theta}, \boldsymbol{\theta}')\varphi_i(\boldsymbol{\theta}'), \varphi_k(\boldsymbol{\theta})] = \int \int_\Theta F(\boldsymbol{\theta}, \boldsymbol{\theta}')\varphi_i(\boldsymbol{\theta}')\varphi_k(\boldsymbol{\theta})\, \mathrm{d}\boldsymbol{\theta}'\, \mathrm{d}\boldsymbol{\theta}, \quad k, i = 1, \ldots, K \tag{3}$$

In the simplest case of applying the regular plane (i.e. equidistant 2-D rectangular) image sampling scheme [16], the two-dimensional δ-basis is applied, in which case the relevant image vectors are simply composed with the lexicographically ordered image samples by stacking either the rows or columns of each discrete plane image into a vector. Assuming that the original sampled image is of support $N\times N$, than these vectors have supports $K\times 1$, where $K = N^2$, and the PSF matrix $\mathbf{F}$ represents the $K\times K$ superposition blur operator. When utilizing the stationary model for the blur, i.e. $F(\boldsymbol{\theta}, \boldsymbol{\theta}') = F(\boldsymbol{\theta} - \boldsymbol{\theta}')$, $\mathbf{F}$ becomes a block-Toeplitz circulant matrix representing the linear spatial convolution-form blur operator [19]. More sophisticated quantification methods, which are also applicable for spatially varying PSF, employ the wavelets with special approximation properties as the basis for image representation in both one- and two-dimensional image scenes [25]. Applying any of these quantification schemes, the continuous-form image formation model (1) is transformed to the relevant K-D vector form

$$\mathbf{u} = \mathbf{F}\mathbf{v} + \mathbf{n}, \tag{4}$$

where the elements of the degraded image vector $\mathbf{u}$, original image vector $\mathbf{v}$, noise vector $\mathbf{n}$ and discrete-form PSF (system blur matrix) $\mathbf{F}$ are defined by inner products (2) and (3), respectively. Eq. (4) is recognized to be a well-known linear image degradation equation. The degraded image $\mathbf{u}$ is viewed as a rough estimate of the original image vector $\mathbf{v}$ formed by the system.

Let us consider now M different degraded images $\mathbf{u}^{(1)}, \ldots, \mathbf{u}^{(M)}$ of the *same* original image $\mathbf{v}$ obtained with M different imaging systems or methods. System or method fusion, as addressed here, utilizes a mathematical model of the mechanism that seeks to apply the aggregate inverse procedure to restore the original image from the data $\mathbf{u}^{(1)}, \ldots, \mathbf{u}^{(M)}$. In the system fusion problem, we associate M different models of the PSFs with the corresponding image formation systems. In the method fusion problem, we assume one given system but apply M different image formation algorithms to acquire the images $\mathbf{u}^{(1)}, \ldots, \mathbf{u}^{(M)}$, respectively. In both cases, instead of one equation (4) we have the system of M equations

$$\mathbf{u}^{(m)} = \mathbf{F}^{(m)}\mathbf{v} + \mathbf{n}^{(m)}, \quad m = 1, \ldots, M \tag{5}$$

with M different PSFs $\mathbf{F}^{(m)}$ and different noise vectors $\mathbf{n}^{(m)}; m = 1, \ldots, M$, respectively, with the further assumption that these zero mean (not necessarily Gaussian) noises are uncorrelated from system to system.

The fusion problem that we consider here is stated as an inverse problem of restoration of the original image $\mathbf{v}$ from M actually formed degraded images $\mathbf{u}^{(m)}$, given the systems' PSFs $\mathbf{F}^{(m)}, m = 1, \ldots, M$. No detailed prior knowledge about probabilistic models of the data is implied, thus a priori model uncertainity is assumed conventional for the practical remote sensing scenarios.

2.2. ME regularization

It is well known that the PSFs are ill-conditioned for practical passive image formation systems [5,6]. Moreover, the statistical uncertainties about an original image and noise significantly complicate the fusion problem making the statistically optimal Bayesian inference techniques [20,24] inapplicable. Hence, a robust deterministic regularization-based approach should be applied when dealing with the formulated above problem. The idea of regularization is to seek for a feasible solution $\hat{\mathbf{v}}$, which, on one hand, provides maximum fidelity to the data minimizing some integrate measure of total energy of the residual error between the models $\mathbf{F}^{(m)}\mathbf{v}$ and the degraded images $\mathbf{u}^{(m)}$, and, on the other hand, the solution should be continuous, i.e. well conditioned with respect to noise fluctuations [11]. The basic feature of regularization is the introduction of a compromise between fidelity to the data and fidelity to some prior information about the solution [3,12]. Dependent on the approach of introducing prior information, the regularization methods can be categorized into two general classes: parametrical model-based and non-parametrical. The first approach uses some low-order parametrical model for data approximation (e.g. ARMA model [12], exponential Prony's model [4], different polynomial approximations [9,26], etc.), in which case the image restoration problem is reduced to the well-posed problem of model identification and parameter estimation. These methods imply a high level of confidence to the used parametrical representation of the data, moreover, the selection of a particular model is the crucial and ambiguous item in the parametrical approximation-based regularization [4,9].

In remote sensing imagery, we generally cannot use the parametrical models of the environmental data at all because of prior uncertainty concerning the scenes, which were actually sensed [14], hence, the non-parametric regularization techniques should be applied. Among such methods [5,6,15,16], the ME regularization approach is recognized to be one of the most grounded because maximizing the entropy as a prior is the most consistent method (in the information theory sense) of selecting a single image from the many images that fit the data [22]. These items were widely discussed in the literature, e.g. [6,15,20,22,25], that is why we do not detail them here and make preference to the ME regularization method, in which the prior information about the image is associated with maximization of the image entropy.

According to an ME model [2,6], the whole image is viewed as a composition of a great amount of elementary discrete counts (speckles or pixels) with the elementary "pixel brightness" β. Every particular image value is represented as a digital pixel

value, i.e. $v_k = \eta_k \beta; k = 1, \ldots, K$, where η_k is a number of counts in the kth image pixel. The total number of pixel counts in a whole image is assumed to be preserved constant, i.e. $\sum_{k=1}^{K} \eta_k = \text{const}$, hence, the total image brightness is kept constant as well, $\sum_{k=1}^{K} \eta_k \beta = B$. The normalized pixel values v_k/B are viewed as those representing the relevant values of the hypothetical discrete probability distribution

$$p_k = \frac{v_k}{B}, \quad \sum_{k=1}^{K} p_k = 1 \tag{6}$$

associated with the corresponding image distribution over the scene, $v_k, k = 1, \ldots, K$. This distribution (6) is characterized by entropy

$$H(\mathbf{p}) = -\sum_{k=1}^{K} p_k \ln p_k. \tag{7}$$

The image entropy function $H(\mathbf{v})$ is defined as a structural copy of (7)

$$H(\mathbf{v}) = -\sum_{k=1}^{K} v_k \ln v_k \tag{8}$$

related to $H(\mathbf{p})$ as

$$H(\mathbf{p}) = -\sum_{k=1}^{K} \frac{v_k}{B} \ln \frac{v_k}{B} = c_1 H(\mathbf{v}) - c_2,$$

where $c_1 = 1/B$ and $c_2 = \ln B$ are the normalization constants independent on the particular image vector $\mathbf{v}$. The ME image model implies the maximum of uncertainity about the probabilistic distribution (6) of the image over the scene. Viewed as a priori information for restoration, the ME model is formalized by imposing the requirement of the maximization of entropy $H(\mathbf{p})$, hence, maximization of the image entropy function $H(\mathbf{v})$ or minimization of its negative value, $-H(\mathbf{v})$.

2.3. Regularization formalism of the system fusion problem

In the aggregate regularization approach that we address here, the contrivance for combining the image restoration problems when performing system fusion is the formation of the augmented cost function

$$E(\mathbf{v}|\boldsymbol{\lambda}) = -\lambda_0 H(\mathbf{v}) + \frac{1}{2}\sum_{m=1}^{M} \lambda_m J_m(\mathbf{v}) + \frac{1}{2}\lambda_{M+1} J_{M+1}(\mathbf{v}), \tag{9}$$

and seeking for a solution $\hat{\mathbf{v}}$ that minimizes the cost (9). Here, $H(\mathbf{v})$ is the image entropy introduced by (8), $\lambda_0, \lambda_1, \ldots, \lambda_M, \lambda_{M+1}$ represent the weight parameters, commonly referred to as the regularization parameters, and $J_m(\mathbf{v})$ are the partial error functions defined as the squares of the l_2 norms of the discrepancies between the actually formed degraded images and the noise-free models of the blurred

images, respectively,

$$J_m(\mathbf{v}) = \|\mathbf{u}^{(m)} - \mathbf{F}^{(m)}\mathbf{v}\|^2 = \left(\mathbf{u}^{(m)} - \mathbf{F}^{(m)}\mathbf{v}\right)^{\mathrm{T}}\left(\mathbf{u}^{(m)} - \mathbf{F}^{(m)}\mathbf{v}\right), \quad m = 1, \ldots, M. \tag{10}$$

The last term $J_{M+1}(\mathbf{v})$ in (9) is a conventional Tikhonov's stabilizer [12] that formalizes prior model assumptions about the "visual quality" of the desired image and is defined as the weighted squared norm

$$J_{M+1}(\mathbf{v}) = \|\mathbf{v}\|_{\mathbf{P}}^2 = (\mathbf{L}\mathbf{v})^{\mathrm{T}}\mathbf{L}\mathbf{v} = \mathbf{v}^{\mathrm{T}}\mathbf{P}\mathbf{v}, \tag{11}$$

which naturally makes the selection of the weight matrix $\mathbf{P} = \mathbf{L}^{\mathrm{T}}\mathbf{L}$ problem dependent. This term imposes a smoothness constraint, which suggests that most images are relatively flat with limited spatial high-frequency activity [16], and thus it is appropriate to minimize the amount of high-pass energy in the restored image. To make the term $J_{M+1}(\mathbf{v})$ represent the squared norm of the high-frequency image components, matrix $\mathbf{L}$ in (11) should be a numerical approximation of the Laplacian operator $\Lambda = \partial^2/\partial\boldsymbol{\theta}^2$ [9]. Applying the general approximation scheme (2), (3) yields the weight matrix $\mathbf{P}$ in the form of a pseudo differential operator composed with elements P_{ki}; $k, i = 1, \ldots, K$, defined by the inner products, $P_{ki} = [\Lambda\varphi_i(\boldsymbol{\theta}), \Lambda\varphi_k(\boldsymbol{\theta})]$, while for the most simple practical case of regular image sampling, the discrete-form approximation of the Laplacian operator [3] is given by the matrix

$$\mathbf{L} = \begin{bmatrix} 1 & -1 & 0 & 0 & 0 & \ldots \\ -1 & 2 & -1 & 0 & 0 & \ldots \\ 0 & -1 & 2 & -1 & 0 & \ldots \\ 0 & 0 & -1 & 2 & -1 & \ldots \\ 0 & 0 & 0 & -1 & 2 & \ldots \\ \ldots & \ldots & \ldots & \ldots & \ldots & \ldots \end{bmatrix}, \tag{12}$$

in which case $J_{M+1}(\mathbf{v})$ is referred to (in regularization theory [12]) as the Tikhonov's stabilizer of the second order. The sum $\Omega(\mathbf{v}|\lambda_{M+1}) = -\lambda_0 H(\mathbf{v}) + (1/2)\lambda_{M+1}J_{M+1}(\mathbf{v})$ comprises a composed regularizing term in the cost function that stabilizes the solution making it smooth (and therefore continuous [12]). Without any loss of generality, the cost function (9) can be normalized by any positive number, e.g. λ_0. Hence, for the purpose of simplicity, since now we will put the weight of the entropy in the augmented cost (9) equal to unity, $\lambda_0 = 1$.

The next step is to express the cost function (9) in an expanded form making the substitutions for the data $\mathbf{u}^{(m)} = \left(u_1^{(m)} \ \ldots \ u_K^{(m)}\right)^{\mathrm{T}}$ defined by Eqs. (5). Expanding Eq. (9) yields

$$E(\mathbf{v}|\boldsymbol{\lambda}) = \sum_{k=1}^{K} v_k \ln v_k + \frac{1}{2}\sum_{m=1}^{M}\left\{\lambda_m\left[\sum_{j=1}^{K}\left(u_j^{(m)} - \sum_{k=1}^{K}F_{jk}^{(m)}v_k\right)^2\right]\right\} + \frac{1}{2}\lambda_{M+1}\sum_{k=1}^{K}\sum_{i=1}^{K}P_{ki}v_k v_i, \tag{13}$$

where $F_{ik}^{(m)}$ and P_{ik} define the corresponding ikth elements of the PSF matrices $\mathbf{F}^{(m)}$ and pseudo differential operator $\mathbf{P}$, respectively, $i,k=1,\ldots,K$.

Expanding the squared terms in (13) and rearranging the resultant expressions, we can rewrite (13) as

$$E(\mathbf{v}|\boldsymbol{\lambda}) = -\frac{1}{2}\sum_{k=1}^{K}\sum_{i=1}^{K} v_k v_i \left\{ -\sum_{m=1}^{M}\left[\lambda_m \sum_{j=1}^{K} F_{jk}^{(m)} F_{ji}^{(m)}\right] - \lambda_{M+1} P_{ki} \right\} - \sum_{k=1}^{K} v_k \left\{ -\ln v_k + \sum_{m=1}^{M}\left[\lambda_m \sum_{j=1}^{K} F_{jk}^{(m)} u_j^{(m)}\right]\right\} + C_E, \tag{14}$$

where

$$C_E = \frac{1}{2}\sum_{m=1}^{M}\lambda_m\left[\sum_{j=1}^{K}\left(u_j^{(m)}\right)^2\right] \tag{15}$$

is a constant term independent of the image vector.

In the frame of the ME regularization approach to system fusion, the restored image is to be found as a solution of the problem

$$\hat{\mathbf{v}} = \underset{\mathbf{v}}{\operatorname{argmin}}\ E(\mathbf{v}|\boldsymbol{\lambda}) \tag{16}$$

of minimizing the cost function (14) with respect to $\mathbf{v}$ for the assigned (or adjusted) values of the regularization parameters, which compose vector $\boldsymbol{\lambda} = (\lambda_1 \ \ldots \ \lambda_M \ \lambda_{M+1})^{\mathrm{T}}$. The proper selection of $\boldsymbol{\lambda}$ is associated with parametrical control of the fusion process. It is important to note that the ME solution $\hat{\mathbf{v}}$ exists and is guaranteed to be unique for a given $\boldsymbol{\lambda}$ because the surfaces of all functions that compose $E(\mathbf{v}|\boldsymbol{\lambda})$ are convex. Furthermore, the entropy is defined only for the positive values, hence, the ME solution is guaranteed to be positive. But one can deduce that due to the non-linearity of the objective function, the solution of the parametrically controlled image restoration problem (16) will require extremely complex computations and result in the technically intractable fusion scheme if this problem is solved employing the standard direct minimization techniques [5,13].

3. Control of the regularization degrees of freedom

3.1. Problem aggregation

The regularization parameters $\lambda_1,\ldots,\lambda_M,\lambda_{M+1}$ (real-valued non-negative numbers) determine the relative importance of the partial terms in the composed cost $E(\mathbf{v}|\boldsymbol{\lambda})$ viewed as a function of the desired image $\mathbf{v}$ subject to the given (assigned) vector $\boldsymbol{\lambda}$. These parameters control the tradeoff between fidelity to the data (as expressed by the terms $J_m(\mathbf{v})$) and smoothness of the solution (as expressed by $\Omega(\mathbf{v}) = \Omega(\mathbf{v}|\lambda_{M+1})$). In remote sensing imagery, parameter λ_{M+1} is always chosen empirically and placed relatively small ($\lambda_{M+1} \sim 10^{-1}-10^{-4}$), because a preference should be given to the measurement data and ME model information [6,9]. Assigning $\lambda_{M+1}=0$, we simply do not require suppression of the high-frequency

image activity imposed by the Tikhonov's stabilizer implying that the model requirements to the "visual quality" of the restored image are fully expressed by the entropy term in the augmented cost function. Control of the other regularization parameters provides additional degrees of freedom of the fusion method. The more value we assign to parameter λ_m, the more weight we assign for the relevant error measure $J_m(\mathbf{v})$, hence, the greater credibility to the actually acquired image (measurement data) and lower importance of the prior image model are assumed. Note, that system fusion tasks are meaningful only in that case when the fidelity to the actually used measurement data is implied to be undoubtedly high and prevail over the weight of a priori information.

When assigning the particular values to the regularization parameters, the question of their preferred selection arises. In the conventional empirical decentralized fusion approach [13], the data acquired by partial systems are usually aggregated with equal weights, thus no optimization mechanism for control of the regularization degrees of freedom is employed. In this section, we develop a method for system data weighting that permits to optimize the balance between the attained spatial resolution and residual noise in the fused image.

Let us define a new set of regularization parameters ω, π_m related to λ_m as

$$\lambda_m = \pi_m \frac{1}{\omega}, \quad \sum_{m=1}^{M} \lambda_m = \frac{1}{\omega}, \quad \sum_{m=1}^{M} \pi_m = 1, \quad m = 1, \ldots, M, \tag{17}$$

and associate the degrees of freedom of the fusion problem with the sum parameter ω^{-1} and vector $\boldsymbol{\pi} = (\pi_1 \ \ldots \ \pi_M)^{\mathrm{T}}$ of the normalized weight parameters $\pi_m, 0 \leqslant \pi_m \leqslant 1$.

Next, to represent the aggregate formalism of the initial fusion problem (16), let us compose the data and noise into the $KM \times 1$ block vectors $\tilde{\mathbf{u}}$ and $\tilde{\mathbf{n}}$ as follows:

$$\tilde{\mathbf{u}} = \left(\mathbf{u}^{(1)\mathrm{T}} \ \ldots \ \mathbf{u}^{(M)\mathrm{T}}\right)^{\mathrm{T}}, \quad \tilde{\mathbf{n}} = \left(\mathbf{n}^{(1)\mathrm{T}} \ \ldots \ \mathbf{n}^{(M)\mathrm{T}}\right)^{\mathrm{T}} \tag{18}$$

and summarize the systems in the aggregate $KM \times M$ system operator composed as

$$\tilde{\mathbf{F}} = \left(\mathbf{F}^{(1)\mathrm{T}} \ \ldots \ \mathbf{F}^{(M)\mathrm{T}}\right)^{\mathrm{T}}. \tag{19}$$

Let $\boldsymbol{\Pi}$ represents the $KM \times KM$ block-diagonal weight matrix,

$$\boldsymbol{\Pi} = \mathrm{blockdiagonal}\{\pi_1 \mathbf{I}, \ldots, \pi_M \mathbf{I}\}. \tag{20}$$

Using definitions (17)–(20), we may rewrite Eq. (9) for the cost function as follows:

$$E(\mathbf{v}|\boldsymbol{\lambda}) = E(\mathbf{v}|\boldsymbol{\pi}, \omega) = \tfrac{1}{2}\left(\tilde{\mathbf{u}} - \tilde{\mathbf{F}}\mathbf{v}\right)^{\mathrm{T}} \boldsymbol{\Pi} \left(\tilde{\mathbf{u}} - \tilde{\mathbf{F}}\mathbf{v}\right) + \omega \boldsymbol{\Omega}(\mathbf{v}). \tag{21}$$

The fusion problem in the aggregate form can now be reformulated as the variational problem

$$\inf_{\mathbf{v}, \omega, \pi} \left\{ \tfrac{1}{2}\left(\tilde{\mathbf{u}} - \tilde{\mathbf{F}}\mathbf{v}\right)^{\mathrm{T}} \boldsymbol{\Pi} \left(\tilde{\mathbf{u}} - \tilde{\mathbf{F}}\mathbf{v}\right) + \omega \boldsymbol{\Omega}(\mathbf{v}) : \mathbf{v} \in V, \tilde{\mathbf{u}} \in \tilde{U} | \omega \geqslant 0, \ \boldsymbol{\pi} \in \Pi \right\} \tag{22}$$

$$\Pi = \left\{ \pi : 0 \leqslant \pi_m \leqslant 1; m = 1, \ldots, M, \sum_{m=1}^{M} \pi_m = 1 \right\},$$

which naturally makes the selection of parameters ω, $\boldsymbol{\pi}$ problem dependent. We are now interested in optimizing such a selection, based on the analysis of the dependence of the performances of optimal solution $\hat{\mathbf{v}}$ of problem (22) on ω, $\boldsymbol{\pi}$.

3.2. Statistical adjustment of the regularization parameters

Hypothesize, first, the standard randomized model of the aggregate data, $\tilde{\mathbf{u}} = \tilde{\mathbf{F}}\mathbf{v} + \tilde{\mathbf{n}}$, characterized by the image mean vector $\mathbf{m}_{\mathbf{v}} = \langle \mathbf{v} \rangle$, image covariance matrix $\mathbf{R}_{\mathbf{v}} = \langle (\mathbf{v} - \mathbf{m}_{\mathbf{v}})(\mathbf{v} - \mathbf{m}_{\mathbf{v}})^{\mathrm{T}} \rangle$, and zero-mean noise with the correlation matrix $\mathbf{R}_{\tilde{\mathbf{n}}}$. In that case, the least-mean squares (LMS) fusion strategy leads to the Bayesian LMS linear optimal restoration [13], $\hat{\mathbf{v}}_{\mathrm{B}} = \mathbf{m}_{\mathbf{v}} + \mathbf{Q}_{\mathrm{B}}(\tilde{\mathbf{u}} - \tilde{\mathbf{F}}\mathbf{m}_{\mathbf{v}})$, with the Bayesian restoration operator $\mathbf{Q}_{\mathrm{B}} = \left(\tilde{\mathbf{F}}^{\mathrm{T}} \mathbf{R}_{\tilde{\mathrm{n}}}{}^{-1} \tilde{\mathbf{F}} + \mathbf{R}_{\mathbf{v}}^{-1}\right)^{-1} \tilde{\mathbf{F}}^{\mathrm{T}} \mathbf{R}_{\tilde{\mathrm{n}}}{}^{-1}$.

In practical remote sensing [14], $\mathbf{R}_{\tilde{\mathbf{n}}}$ is usually approximated as $KM \times KM$ block diagonal matrix

$$\mathbf{R}_{\tilde{\mathbf{n}}} \approx \mathbf{N} = \text{block diagonal}\{N_1\mathbf{I}, \ \ldots, N_M\mathbf{I}\}, \tag{23}$$

where N_m represents the noise intensity in the mth degraded image, $m = 1, \ldots, M$. Similarly, for the purposes of analysis, it is conventional to approximate $\mathbf{R}_{\mathbf{v}}$ as $K \times K$ diagonal matrix [14]:

$$\mathbf{R}_{\mathbf{v}} \approx (v_0)^2 \mathbf{I}, \tag{24}$$

where $v_0 = (1/K) \sum_{k=1}^{K} v_k$ represents the average gray level of the image. Taking these approximations, the Bayesian linear restoration operator becomes simply

$$\mathbf{Q}_{\mathrm{B}} = \left(\tilde{\mathbf{F}}^{\mathrm{T}} \mathbf{N}^{-1} \tilde{\mathbf{F}} + (v_0)^{-2} \mathbf{I}\right)^{-1} \tilde{\mathbf{F}}^{\mathrm{T}} \mathbf{N}^{-1}. \tag{25}$$

It is well known that Bayesian solution $\hat{\mathbf{v}}_{\mathrm{B}}$ is characterized by the optimal balance (in the LMS sense) between the gained resolution and noise suppression in the restored image [9].

The regularized fusion approach is formalized by variational problem (22). Although the solution of the problem (22) is nonlinear, associating that with the output of some hypothetical linear restoration filter $\mathbf{Q}_{\omega,\boldsymbol{\pi}} = \mathbf{Q}(\omega, \boldsymbol{\pi})$, the selection of the filter's parameters ω, $\boldsymbol{\pi}$ can be optimized in such a fashion that $\mathbf{Q}_{\omega,\boldsymbol{\pi}}$ provides an approximation to the Bayesian operator (25), in which case the resolution-to-noise balance in the actual fused image $\hat{\mathbf{v}}$ approaches to that attained in the hypothetical Bayesian solution $\hat{\mathbf{v}}_{\mathrm{B}}$. To derive the approximating filter $\mathbf{Q}_{\omega,\boldsymbol{\pi}}$ consider the Euler equation related to the variational problem (22),

$$\tilde{\mathbf{F}}^{\mathrm{T}} \boldsymbol{\Pi} \tilde{\mathbf{F}} \mathbf{v} + \omega \mathbf{f}(\mathbf{v}) = \tilde{\mathbf{F}}^{\mathrm{T}} \boldsymbol{\Pi} \tilde{\mathbf{u}}, \tag{26}$$

where $\mathbf{f}(\mathbf{v}) = \partial \Omega(\mathbf{v}) / \partial \mathbf{v}$ defines the $K \times 1$ gradient vector.

Consider that the solution, $\hat{\mathbf{v}}_{\omega,\boldsymbol{\pi}} = \hat{\mathbf{v}}(\omega,\pi)$, of Eq. (26) is found and is close (for the properly chosen ω, $\boldsymbol{\pi}$) to the true image $\mathbf{v}$, i.e. we may approximately express

$$\mathbf{f}\big(\hat{\mathbf{v}}_{\omega,\boldsymbol{\pi}}\big) - \mathbf{f}(\mathbf{v}) \approx \mathbf{A}_{\hat{\mathbf{v}}(\omega,\boldsymbol{\pi})}\big(\hat{\mathbf{v}}_{\omega,\boldsymbol{\pi}} - \mathbf{v}\big) \approx \mathbf{A}_{\mathbf{v}}\big(\hat{\mathbf{v}}_{\omega,\boldsymbol{\pi}} - \mathbf{v}\big), \tag{27}$$

where $\mathbf{A}_{\hat{\mathbf{v}}(\omega,\boldsymbol{\pi})}$, $\mathbf{A}_{\mathbf{v}}$ are the $K\times K$ matrices, $\mathbf{A}_{\hat{\mathbf{v}}(\omega,\boldsymbol{\pi})} = \partial\mathbf{f}(\hat{\mathbf{v}}_{\omega,\boldsymbol{\pi}})/\partial\hat{\mathbf{v}}_{\omega,\boldsymbol{\pi}}$ and $\mathbf{A}_{\mathbf{v}} = \partial\mathbf{f}(\mathbf{v})/\partial\mathbf{v}$, respectively. If $\hat{\mathbf{v}}_{\omega,\boldsymbol{\pi}}$ is a solution of the Euler equation (26) (e.g. one found applying the NN-based method, to be presented in the next section) then using approximations (27) and representing $\tilde{\mathbf{u}} = \tilde{\mathbf{F}}\mathbf{v} + \tilde{\mathbf{n}}$, we can rewrite Eq. (26) as

$$\Big(\tilde{\mathbf{F}}^{\mathrm{T}}\boldsymbol{\Pi}\tilde{\mathbf{F}} + \omega\mathbf{A}_{\hat{\mathbf{v}}(\omega)}\Big)\hat{\mathbf{v}}_{\omega} \approx \Big(\tilde{\mathbf{F}}^{\mathrm{T}}\boldsymbol{\Pi}\tilde{\mathbf{F}} + \omega\mathbf{A}_{\hat{\mathbf{v}}(\omega)}\Big)\mathbf{v} - \mathbf{f}\big(\hat{\mathbf{v}}_{\omega,\boldsymbol{\pi}}\big) + \tilde{\mathbf{F}}^{\mathrm{T}}\boldsymbol{\Pi}\tilde{\mathbf{n}},$$

that yields

$$\hat{\mathbf{v}}_{\omega,\boldsymbol{\pi}} \approx \mathbf{v} - \Big(\tilde{\mathbf{F}}^{\mathrm{T}}\boldsymbol{\Pi}\tilde{\mathbf{F}} + \omega\mathbf{A}_{\hat{\mathbf{v}}(\omega,\boldsymbol{\pi})}\Big)^{-1}\mathbf{f}\big(\hat{\mathbf{v}}_{\omega,\boldsymbol{\pi}}\big) + \Big(\tilde{\mathbf{F}}^{\mathrm{T}}\boldsymbol{\Pi}\tilde{\mathbf{F}} + \omega\mathbf{A}_{\hat{\mathbf{v}}(\omega,\boldsymbol{\pi})}\Big)^{-1}\tilde{\mathbf{F}}^{\mathrm{T}}\boldsymbol{\Pi}\tilde{\mathbf{n}} \tag{28}$$

Next, associating the regularizing term with the image entropy, $\Omega(\mathbf{v}) = -H(\mathbf{v}) = \sum_{k=1}^{K} v_k \ln v_k$, the approximation to $\mathbf{A}_{\hat{\mathbf{v}}(\omega,\boldsymbol{\pi})}$ can be represented as

$$\mathbf{A}_{\hat{\mathbf{v}}(\omega,\boldsymbol{\pi})} \approx \mathbf{A}_{\mathbf{v}} = \frac{\partial\mathbf{f}(\mathbf{v})}{\partial\mathbf{v}} = \frac{\partial^2\Omega(\mathbf{v})}{\partial\mathbf{v}^2} = \mathrm{diag}\big\{v_1^{-1},\ldots,v_K^{-1}\big\} \approx (1/v_0)\mathbf{I} \tag{29}$$

Using approximation (29), Eq. (28) may be rewritten in the following compact form:

$$\hat{\mathbf{v}}_{\omega,\boldsymbol{\pi}} \approx \mathbf{v} - \mathbf{v}_s + \mathbf{Q}_{\omega,\boldsymbol{\pi}}\tilde{\mathbf{n}}, \tag{30}$$

where

$$\mathbf{Q}_{\omega,\boldsymbol{\pi}} = \Big(\tilde{\mathbf{F}}^{\mathrm{T}}\boldsymbol{\Pi}\tilde{\mathbf{F}} + \omega/v_0\mathbf{I}\Big)^{-1}\tilde{\mathbf{F}}^{\mathrm{T}}\boldsymbol{\Pi}, \tag{31}$$

the term, $\mathbf{v}_s = \Big(\tilde{\mathbf{F}}^{\mathrm{T}}\boldsymbol{\Pi}\tilde{\mathbf{F}} + \omega/v_0\mathbf{I}\Big)^{-1}\mathbf{f}\big(\hat{\mathbf{v}}_{\omega,\boldsymbol{\pi}}\big)$, pertains to a systematic error in the restored image due to finite resolution, while the term, $\mathbf{Q}_{\omega,\boldsymbol{\pi}}\tilde{\mathbf{n}}$, counts to the noise component in the solution. The impact of noise is characterized by the noise error measure (noise energy)

$$\rho_n(\omega,\boldsymbol{\pi}) = \Big\langle \|\mathbf{Q}_{\omega,\boldsymbol{\pi}}\tilde{\mathbf{n}}\|^2 \Big\rangle = \mathrm{trace}\Big\{\mathbf{Q}_{\omega,\boldsymbol{\pi}}\mathbf{R}_{\mathbf{n}}\mathbf{Q}_{\omega,\boldsymbol{\pi}}^{\mathrm{T}}\Big\}. \tag{32}$$

This measure (32) is recognized to be the same one as that for the corresponding noise energy at the output of a hypothetical linear restoration filter $\mathbf{Q}_{\omega,\boldsymbol{\pi}}$ applied to the aggregate data $\tilde{\mathbf{u}}$ [13]. Thus viewing (31) as an approximation to the linear Bayesian restoration filter (24), yields the following statistical scheme for selection of the regularization parameters:

$$\hat{\pi}_m = v_0\left(N_m\sum_{j=1}^{M} v_0/N_j\right)^{-1}, \quad \hat{\omega}\left(\sum_{j=1}^{M} v_0/N_j\right)^{-1}, \ \hat{\lambda}_m = v_0/N_m, \quad m = 1,\ldots,M, \tag{33}$$

in which case two filters (25) and (31) coincide. The main problem with this approach is that the knowledge of the average image gray level v_0 and noise intensities N_m is needed to compute the estimates (33). In order to pre-estimate these parameters, we must have access to the sensors and rather substantial calibration experiments must be carried out.

3.3. Use of calibration data

According to statistical scheme (33), regularization parameters λ_m are selected proportionally to the expected image average gray value v_0 and inversely proportional to noise intensities N_m in the corresponding degraded images, $m = 1, \ldots, M$. The empirical adjustment of parameters λ_m that approaches the scheme (33) could be performed based on the use of the systems calibration data. Before utilizing passive sensing systems, their calibration is performed by measuring the systems' signal-to-noise ratios (SNR)

$$\Gamma^{(m)} = \frac{\left\langle \|\mathbf{s}_0^{(m)}\|^2 \right\rangle}{\left\langle \|\mathbf{n}^{(m)}\|^2 \right\rangle} = \frac{\left\langle \|\mathbf{F}^{(m)}\mathbf{v}_0 + \mathbf{n}^{(m)}\|^2 \right\rangle - \left\langle \|\mathbf{n}^{(m)}\|^2 \right\rangle}{\left\langle \|\mathbf{n}^{(m)}\|^2 \right\rangle}, \quad m = 1, \ldots, M, \tag{34}$$

where $\Gamma^{(m)}$ is the average SNR at the output of the mth imaging system measured by some means [8,14] for the applied calibration input $\mathbf{v}_0$(e.g. $\mathbf{v}_0 = v_0\mathbf{1}$), and $\langle\cdot\rangle$ denotes the ensemble average. Viewed as approximation to the ratios, v_0/N_m, measurements (34) can be used to adjust the corresponding regularization parameters

$$\hat{\pi}_m = \Gamma^{(m)} \left(\sum_{j=1}^{M} \Gamma^{(j)} \right)^{-1}, \quad \hat{\omega} = \left(\sum_{j=1}^{M} \Gamma^{(j)} \right)^{-1}, \quad \hat{\lambda}_m = \Gamma^{(m)}, \quad m = 1, \ldots, M, \tag{35}$$

that approximate the statistical selection scheme (33).

3.4. Resolution-to-noise balance

Statistical scheme (33) and its calibration data-based approximation (35) provide no availability to balance between the gained spatial resolution and noise suppression in the resultant restored image. In practice, it is sometimes tempting to permit higher noise level if we are interested in attaining the enhanced spatial resolution. In that case, we have to select the regularization parameters in such a fashion that the systematic error in the restored image is minimized (i.e. spatial resolution is maximized) subject to the constraint that the noise error is bounded by some prescribed admissible level. Using approximations (23) and (24), we further represent the noise error measure (32) as follows:

$$\begin{aligned} \rho_n(\omega, \pi) &= \operatorname{trace}\left\{ \left(\tilde{\mathbf{F}}^{\mathrm{T}} \mathbf{\Pi} \tilde{\mathbf{F}} + \omega/v_0 \mathbf{I} \right)^2 \tilde{\mathbf{F}}^{\mathrm{T}} \mathbf{\Pi} \mathbf{N} \mathbf{\Pi} \tilde{\mathbf{F}} \right\} \\ &\approx N_0 \operatorname{trace}\left\{ \left(\tilde{\mathbf{F}}^{\mathrm{T}} \mathbf{\Pi} \tilde{\mathbf{F}} + \omega/v_0 \mathbf{I} \right)^{-2} \tilde{\mathbf{F}}^{\mathrm{T}} \mathbf{\Pi}^2 \tilde{\mathbf{F}} \right\}, \end{aligned} \tag{36}$$

where approximation, $\mathbf{N} = N_0\mathbf{I}$, was made for the case of prior unknown noise intensities N_m by substituting those with the average intensity $N_0 = (1/M)\sum_{m=1}^{M} N_m$.

The systematic error measure in the fused image (30) is now expressed by

$$\rho_s(\omega, \pi) = \left\langle \|\mathbf{v}_s\|^2 \right\rangle \approx \operatorname{trace}\left\{ (1 + \ln v_0)^2 \left(\tilde{\mathbf{F}}^{\mathrm{T}} \mathbf{\Pi} \tilde{\mathbf{F}} + \omega/v_0 \mathbf{I} \right)^{-2} \right\}. \tag{37}$$

For a fixed $\boldsymbol{\pi}$, the noise error measure $\rho_n(\omega, \boldsymbol{\pi})$ defined by Eq. (36) is a monotonic decreasing function of parameter ω, while the systematic error measure $\rho_s(\omega, \pi)$ given by (37) is an increasing function of ω. Hence, the resolution-to-noise balance can be efficiently controlled by this regularization degree of freedom. We have to pre-select the weight parameters $\hat{\pi}_m = \Gamma^{(m)}\left(\sum_{j=1}^{M}\Gamma^{(j)}\right)^{-1}$; $m = 1, \ldots, M$ (e.g. using empirical calibration-based scheme (35)), fix the noise in the fused image at some admissible level δ and choose ω as a solution to the balance equation,

$$N_0 \operatorname{trace}\left\{\left(\tilde{\mathbf{F}}^{\mathrm{T}}\boldsymbol{\Pi}\tilde{\mathbf{F}} + \omega/v_0\mathbf{I}\right)^{-2}\tilde{\mathbf{F}}^{\mathrm{T}}\boldsymbol{\Pi}^2\tilde{\mathbf{F}}\right\} = \delta. \tag{38}$$

For example, if resolution-to-noise balance factor δ is selected as, $\delta = \operatorname{trace}\{\hat{\mathbf{R}}_{\tilde{\mathbf{n}}}\} \approx N_0 KM$, then solution $\hat{\omega}$ of the balance equation (38) adjusts the regularization parameters

$$\hat{\lambda}_m = \hat{\omega}^{-1}\hat{\pi}_m, \quad m = 1, \ldots, M, \tag{39}$$

to maximize spatial resolution in the fused image subject to the constraint that noise does not exceed the average level that it exposes in the actually acquired degraded images. The resultant measures of the noise and systematic errors are now balanced at their values, $\rho_n(\hat{\boldsymbol{\lambda}})$ and $\rho_s(\hat{\boldsymbol{\lambda}})$, defined by Eqs. (36) and (37), respectively, for the estimated values (39) of the regularization parameters.

4. Neural network for image restoration with system fusion

4.1. Model of the multistate Hopfield-type NN

The multistate Hopfield-type NN is a massive interconnection of formal neurons as basic processing units as depicted in Fig. 1. The states x_k; $k = 1, \ldots, K$ of all K neurons of the multistate NN may take values in a range from 0 (black level) to some pre-assigned maximum value X (white level). These values are used to represent the gray levels of the image in the process of restoration. The initial state of a neuron k is denoted as x_k^0. Each neuron k is visited *sequentially* in discrete time. The feedback loops involve the use of particular branches composed of unit-delay elements (in Fig. 1(b) these are denoted by τ). At each particular visit, a neuron k receives at its ith input node the input signal $a_{ki} = x_i$ that is just the current state of the ith neuron, $i = 1, \ldots, K$, and a bias input θ_k at its $(K+1)$st (bias) node. Thus, each neuron receives the signals from all other neurons including itself and a bias input. The outputs of all K neurons

$$z_k = \operatorname{sgn}\left(\sum_{i=1}^{K} W_{ki}a_{ki} + \theta_k\right) = \operatorname{sgn}\left(\sum_{i=1}^{K} W_{ki}x_i + \theta_k\right), \quad k, i = 1, \ldots, K \tag{40}$$

compose the output vector, $\mathbf{z} = \operatorname{sgn}(\mathbf{W}\mathbf{x} + \boldsymbol{\theta})$, where $\mathbf{W}$ is the $K \times K$ matrix of the interconnection strengths (synaptic weights W_{ki}) of the NN, and $\boldsymbol{\theta}$ is the $K \times 1$ bias vector. The output vector $\mathbf{z}$ is used to update the state vector $\mathbf{x} = (x_1\ x_2\ \ldots\ x_K)^{\mathrm{T}}$ of

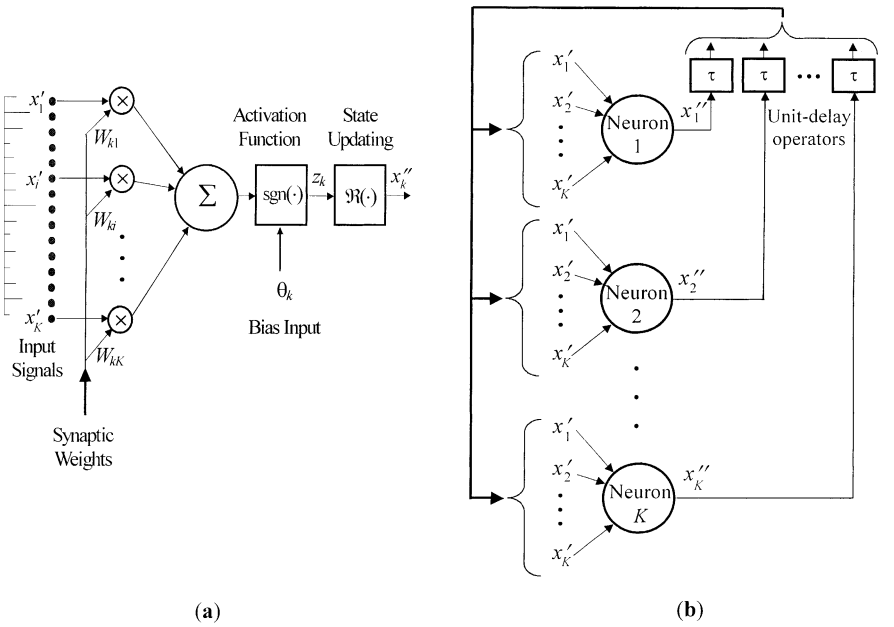

Fig. 1. Multistate NN for imaging system fusion: (a) structure of kth neuron; (b) NN's structure.

the network: $\mathbf{x}''=\mathbf{x}'+\Delta\mathbf{x}$, where $\Delta\mathbf{x}=\Re(\mathbf{z})$ is a change of the state vector $\mathbf{x}$ that is computed by applying some state update rule $\Re(\mathbf{z})$ and the superscripts $'$ and $''$ correspond to the state values before and after network state updating, respectively. The energy function [10] of the network is defined as

$$E=-\frac{1}{2}\mathbf{x}^{\mathrm{T}}\mathbf{W}\mathbf{x}-\boldsymbol{\theta}^{\mathrm{T}}\mathbf{x}=-\frac{1}{2}\sum_{k=1}^{K}\sum_{i=1}^{K}W_{ki}x_kx_i-\sum_{k=1}^{K}\theta_kx_k. \tag{41}$$

If the state update rule $\Re(\mathbf{z})$ is properly designed, then the decrease of the energy function (41) is guaranteed at each updating step, i.e. $E''\leqslant E'$, until finally the energy function E converges to its some stable minimal value $E_{\min}$ that is referred to as the stationary point of the network. Thus, the operational features of the multistate NN depend on: (1) the values assigned to the matrix of the interconnection strengths $\mathbf{W}$ and bias vector $\boldsymbol{\theta}$; (2) the employed state update rule $\Re(\mathbf{z})$.

Clearly, if the energy function of the NN represents the function of a mathematical minimization problem over a parameter space, then the state of the NN would represent the parameters and the stationary point of the network would represent a minimum of the original minimization problem. Hence, utilizing the concept of the Hopfield-type network, we may translate our image restoration problem with system fusion to a relevant problem of minimization of the energy function of a NN.

In this study, we rely on the multistate Li et al.'s MENN proposed in [22] because of its universal computational structure that allows generalization for solving the

mathematical minimization problems with augmented cost functions. The initial Li's MENN was designed to solve the image restoration problem for the case of only one formation system, i.e. $M = 1$. The matrix of interconnection strengths $\mathbf{W}$ and vector of bias inputs $\boldsymbol{\theta}$ of the NN were selected to minimize the cost function

$$E(\mathbf{v}|\boldsymbol{\lambda}) = -H(\mathbf{v}) + \tfrac{1}{2}\lambda_1\|\mathbf{u} - \mathbf{F}\mathbf{v}\|^2 + \tfrac{1}{2}\lambda_2\|\mathbf{D}\mathbf{v}\|^2,$$

where the linear convolution operator $\mathbf{D}$ was defined as a numerical approximation of the Laplacian operator Λ and the regularization parameter λ_1 was adjusted to get feasible solutions that satisfied the imposed fidelity measure [22].

The idea of computational implementation of the proposed aggregate fusion method using a NN is based on the modification of the MENN algorithm *without* complicating the NN's computational structure of Fig. 1 *independent* on a number of systems to be fused. To accomplish this we redefine the NN's operation parameters $\mathbf{W}$, $\boldsymbol{\theta}$ in such a fashion that the new MENN algorithm integrates the model parameters of all M systems that enables the network to perform the fusion. The state update rule is also modified to control the trade-off between the computational complexity and accuracy of finding the stationary point of the network. Implementing the developed MENN algorithm, the values of the regularization parameters may be chosen empirically or controlled applying the selection schemes proposed in Section 3.

4.2. Fused image restoration with MENN

Reconsider now the cost function $E(\mathbf{v}|\boldsymbol{\lambda})$ given by (14) as an energy function of the multistate NN and specify the interconnection strengths W_{ki} and bias inputs θ_k of the network expressing those via the parameters of function $E(\mathbf{v}|\boldsymbol{\lambda})$. By comparing Eqs. (14) and (41) we define

$$W_{ki} = -\sum_{m=1}^{M}\left[\lambda_m \sum_{j=1}^{K} F_{jk}^{(m)} F_{ji}^{(m)}\right] - \lambda_{M+1} P_{ki}, \tag{42}$$

$$\theta_k = -\ln x_k \sum_{m=1}^{M}\left[\lambda_m \sum_{j=1}^{K} F_{jk}^{(m)} y_j^{(m)}\right], \tag{43}$$

where we redenoted $x_k = v_k$, $y_k = u_k$ and ignored the constant term (15) that does not involve $\mathbf{v}$.

Having specified the parameters of the NN, we can apply the direct descent method for minimization of its energy function [10]. Consider one single updating step with particular neuron k. Let Δx_k define a state change of neuron k, i.e. we may express the state of neuron k after updating as $x_k'' = x_k' + \Delta x_k$. The energy function E takes the change $\Delta E = E'' - E'$ due to neuron k updating. Using definition (41), this energy change can be expressed as

$$\Delta E = -\left(\sum_{i=1}^{K} W_{ki} x_i'\right)\Delta x_k - \left(\theta_k'' x_k'' - \theta_k' x_k'\right) - \tfrac{1}{2} W_{kk}(\Delta x_k)^2. \tag{44}$$

The second term on the right-hand side of Eq. (44) may be substantially simplified if we assume that all $x_k \gg 1$:

$$\theta''_k x''_k - \theta'_k x'_k = \theta'_k \Delta x_k + (\theta''_k - \theta'_k) x''_k$$
$$= \theta'_k \Delta x_k + \ln\left(1 - \frac{\Delta x_k}{x''_k}\right) x''_k \approx (\theta'_k - 1)\Delta x_k.$$

This enables us to approximate the energy change

$$\Delta E \approx -\left(\sum_{i=1}^{K} W_{ki} x'_i - \theta'_k - 1\right)\Delta x_k - \tfrac{1}{2} W_{kk} (\Delta x_k)^2$$

and redefine the output (40) of neuron k as follows:

$$z_k = \operatorname{sgn}\left(\sum_{i=1}^{K} W_{ki} x'_i + \theta'_k - 1\right), \quad k = 1, \ldots, K. \tag{45}$$

Now, to guarantee the non-positive values of ΔE, the following state update rule can be applied:

$$\Delta x_k = \Re(z_k) = \begin{cases} 0 & \text{if} \quad z_k = 0, \\ \Delta & \text{if} \quad z_k > 0, \\ -\Delta & \text{if} \quad z_k < 0, \end{cases} \tag{46}$$

where Δ is the preassigned step-size parameter. If no changes of ΔE are examined while approaching to the stationary point of the network, then the step-size parameter Δ may be decreased, which enables one to monitor the updating process as it progresses setting a compromise between the desired accuracy of finding the NN's stationary point and computational complexity. To satisfy the condition $x_k \gg 1$ some constant v^0 may be added to the gray level of every original image pixel and after restoration the same constant should be deducted from the gray level of every restored image pixel, hence, the selection of a particular value of v^0 is not critical. Thus, we revise the model of the degraded images that we employ from M different image formation systems replacing the actually acquired images $\mathbf{u}^{(m)}$ by the renewed data vectors

$$\mathbf{y}^{(m)} = \mathbf{F}^{(m)}(\mathbf{v} + v^0 \mathbf{1}) + \mathbf{n}^{(m)} = \mathbf{u}^{(m)} + v^0 \mathbf{F}^{(m)} \mathbf{1}, \quad m = 1, \ldots, M, \tag{47}$$

where $\mathbf{1} = (1\ 1\ \ldots\ 1)^{\mathrm{T}} \in R^K$ is the $K \times 1$ vector composed with ones. Consequently, the restored image $\hat{\mathbf{v}}$ corresponds to the state vector $\hat{\mathbf{x}}$ of the NN in its stationary point as, $\hat{\mathbf{v}} = \hat{\mathbf{x}} - v^0 \mathbf{1}$.

Here, we provide the iterative algorithm that implements the proposed method. The steps of the algorithm are listed as follows.

Step 1: Make the necessary corrections (47) of the data vectors.

Step 2: Choose suitable values of the regularization parameters $\lambda_m; m = 1, \ldots, M+1$, empirically or applying the schemes developed in Section 3.

Step 3: Compute the weighted vector $\mathbf{y} = (1/\sum_{m=1}^{M} \lambda_m) \sum_{m=1}^{M} \lambda_m \mathbf{y}^{(m)}$ and consider it as the initial state vector $\mathbf{x}^0$ of the neurons; compute the synaptic weights (42) and bias inputs (43) of the NN.

Step 4: Sequentially visit all neurons to complete one iteration. Use the state update rule (46) repeatedly until there are no changes in the energy function. After completing each iteration, update the bias inputs (43).

Step 5: Check the energy function E. If the energy function decreases, return to step 4 for the next iteration. If the energy does not change (ΔE is less than some selected threshold), decrease the step-size parameter Δ 2 times and return to step 4 for the next iteration. Repeat step 5 until the step-size parameter takes some prescribed minimal value $\Delta_{\min}$ or there are no changes in the energy function.

Step 6: Deduct the constant v^0 from the gray level of every pixel of the stationary state vector $\hat{\mathbf{x}}$ of the NN and compute the restored image $\hat{\mathbf{v}} = \hat{\mathbf{x}} - v^0\mathbf{1}$.

When the optimization schemes for selection of the regularization parameters are applied, the result of the restoration becomes a balanced trade-off between the gained spatial resolution and noise suppression in the resultant fused image. Any other measures of misfit are also possible [3,9,22]. In these cases, the second step of the presented algorithm should be revised to perform the necessary adjustment of the regularization parameters. Hence, different modifications of the proposed MENN may also be developed to control its regularization degrees of freedom.

5. Simulation results

This section presents the results of simulations of the developed method carried out in one dimension for the case of fusing the data provided by two different passive radar systems operating in the same frequency waveband and scanning in one direction along the same scene (e.g. two passive imaging radars displaced on one platform or closely adjacent platforms). The systems' PSFs were simulated as the corresponding antennas receiving patterns. The first simulated system uses an equispaced half-wavelength far apart K-element linear antenna array, which performs the conventional linear beamforming [5] to scan electrically over the scene. In simulations, it is sufficient to consider only the main beam and the nearest sidelobes in the PSF, which levels exceed -20 dB because the total power of the signals in all other sidelobes is negligibly small [8]. Thus, the PSF of the first system (see Fig. 2(a)) had four considerable sidelobes, its width at half maximum was 8 pixels of 200-pixel image format and its full width was bounded to 30 pixels.

The second simulated system corresponds to the model of an ultra-low sidelobe antenna with Taylor weighted aperture distribution [8] (see Fig. 2(b)). In that case, less than 1% of the receiving signal power is in sidelobes (hence, in simulations their impact may be ignored) while the decrease in the sidelobes level is accompanied with the relevant widening of the main beam of the antenna pattern. Its width at half maximum was 15 pixels and the full width was bounded to 30 pixels.

The original image was $K = 200$ pixels in size and contained one extended object of 115 pixels width and 5 point-type objects each of 4 pixels width displaced in the image scene as shown in Fig. 3(a). Convoluting the original image with the corresponding PSFs simulated the blurred images. The additive noise vectors were modeled as white $\chi^2(K)$-distributed random vectors (chi-squared discrete Pearson

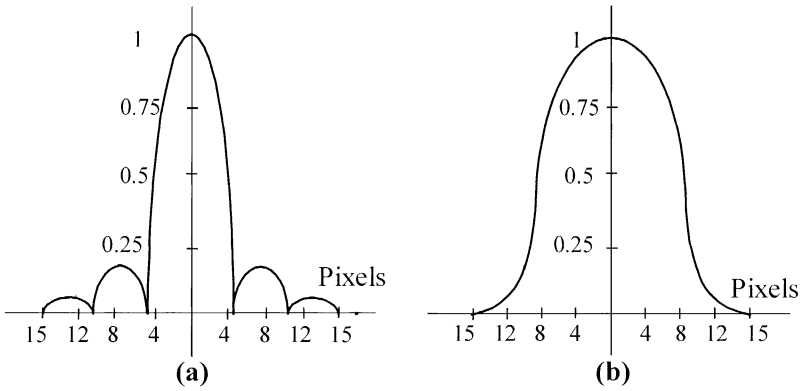

Fig. 2. Simulated PSFs: (a) first system; (b) second system.

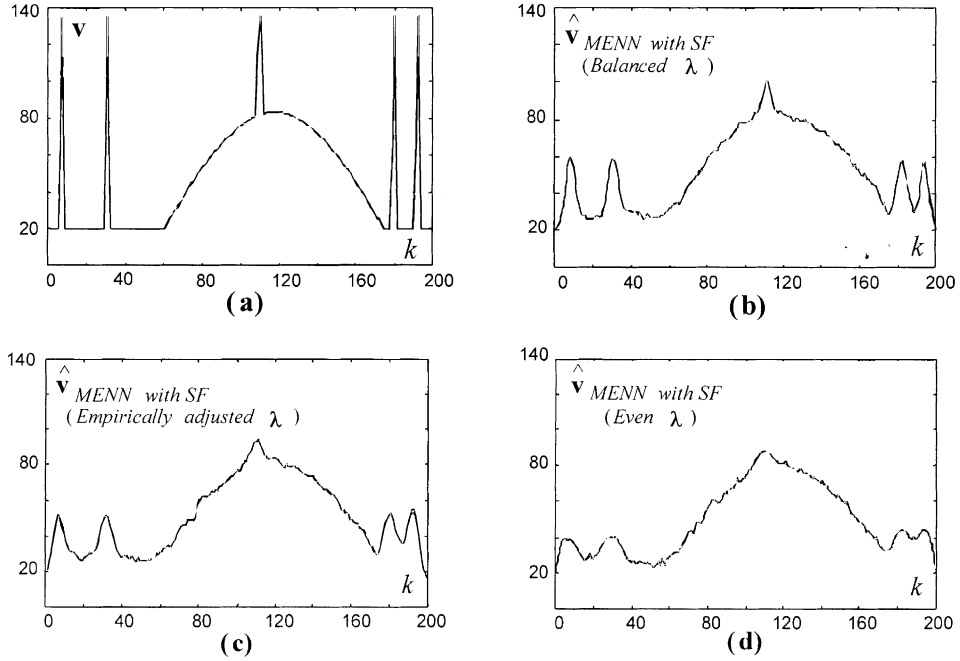

Fig. 3. Simulation results: (a) original simulated image; (b) MENN restoration with system fusion (SF) applying optimally balanced data aggregation; (c) fused MENN restoration with empirically statistically adjusted regularization parameters; (d) fused MENN restoration with evenly assigned weights; (e), (f) degraded images formed by systems 1 and 2, respectively; (g), (h) RLS restoration of two degraded images of (e) and (f), respectively; (k), (l) MENN restoration of two degraded images of (e) and (f), respectively, without system fusion. In all the images, the horizontal axis corresponds to the 1-D image pixel number, while the vertical axis represents the image brightness values.

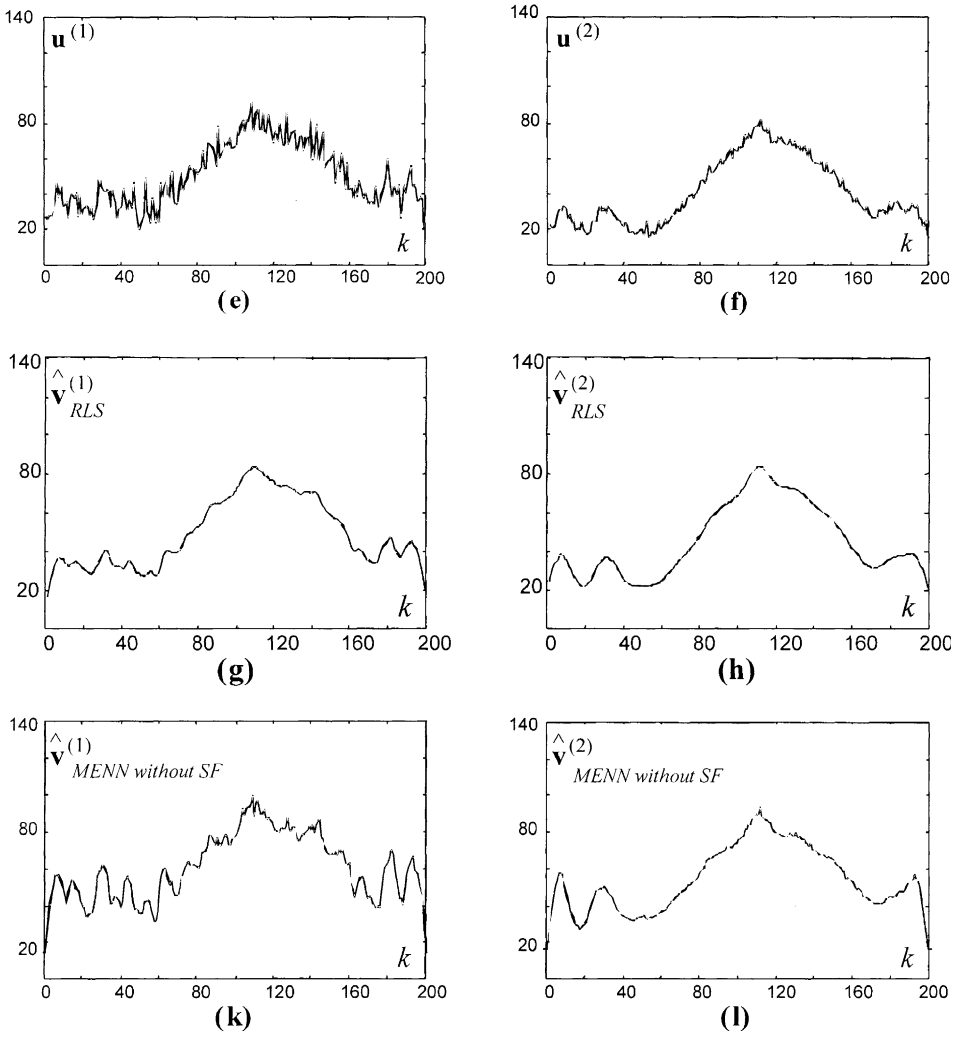

Fig. 3. (*continued*).

noise with K degrees of freedom [3]) as inherent for the passive radar listening systems [5,6] and added to the blurred images. The average noise intensity was put $N_1 = 15$ for the first system and $N_2 = 7$ for the second system, respectively, with the maximum value of the brightness scale $X = 140$. The lower noise level assumed for the second system accounts to the model of the higher signal-to-noise ratio.

To demonstrate the performance of the proposed MENN, we compared it with the Tikhonov's iterative regularized least squares (RLS) restoration algorithm, which does not employ the ME image model [11], and with the MENN without system fusion [22] applied to each of two degraded images separately. We used the

conventional measure [19] of improvement in the signal-to-noise ratio (ISNR),

$$\mu = 10 \log_{10} \frac{\sum_{k=1}^{K} (u_k - v_k)^2}{\sum_{k=1}^{K} (\hat{v}_k - v_k)^2} \tag{48}$$

as a quantitative evaluation of the restoration process. The better restoration process is characterized with the higher ISNR, because the higher μ, the closer is the restored image $\hat{\mathbf{v}}$ to the original image $\mathbf{v}$. To qualify the results of system fusion, the degraded image acquired by the second system was chosen as the reference image, i.e. $\mathbf{u}^{(2)} = \mathbf{u}$, when formula (48) was applied.

The simulation results are presented in Figs. 3(a)–(l). Fig. 3(a) shows the original simulated image. Fig. 3(b) shows the restoration result obtained using the proposed MENN algorithm with the balanced regularization parameters. Parameters $\hat{\pi}_m$ were adjusted applying empirical calibration-based scheme (35), and ω was optimized as a solution to the balance equation (38) for the preassigned noise factor $\delta = N_2 KM$, in which case the MENN algorithm maximized spatial resolution in the fused image with respect to the constraint that noise should not exceed the level that it exposed in the second degraded image. Fig. 3(c) represents the restored image obtained with the same MENN algorithm but for the case of empirically selected λ_1, λ_2 according to statistical scheme (33). Fig. 3(d) shows the result of fused MENN image restoration using robust pre-selected even values of regularization parameters $\lambda_1 = \lambda_2 = 1$ (i.e. no optimization of the regularization parameters was applied). The gray level of the original image before restoration was increased by a constant, $v^0 = 20$. Figs. 3(e) and (f) show the degraded images at the outputs of the first and the second image formation systems, respectively. Figs. 3(g) and (h) show the restoration results obtained by applying the RLS iterative restoration algorithm [11] to the images of Figs. 2(e) and (f), respectively. Figs. 3(k) and (l) represent the restoration results of the Li's MENN method [22] applied independently to the degraded images of Figs. 3(e) and (f), respectively. In all these algorithms, the weight λ_3 of the Tikhonov's stabilizer (12) in the corresponding cost functions was assigned the same value, $\lambda_3 = 10^{-2}$. The iteration process was terminated at the step-size parameter, $\Delta_{\min} = 0.5$, with the initial value $\Delta = 1$.

Analyzing the presented simulation results, we may summarize the following. The RLS method does not provide the qualitative restoration because it is basically a linear inverse filtering technique that employs no specific a priori regularizing information. The MENN without fusion exhibited the good restoration performances for the both systems but the better performances were obtained applying the system fusion: the resolution was improved, all objects were clearly distinguished, and the ringing effect was substantially decreased. In Table 1 we present the values of the ISNR for the iterative RLS algorithm and two neural networks: the first one that employs the Li's MENN algorithm applied separately to the data acquired by the systems, and the second one that implements the developed fusion algorithm with different options of a choice of the regularization parameters, along with the comparison of their convergence rates. The reconstructions proved to be sensitive to the choice of the regularization parameters. For the above simulations reported in

Table 1
ISNR values and number of iterations for three restoration methods: RLS, Li's MENN without system fusion and the proposed method for three different options of a choice of the regularization parameters. Results are presented for two degraded images shown in Figs. 3(e) and (f), respectively

Image restoration using different methods	ISNR	Number of iterations
RLS method: system 1	2.28	30
RLS method: system 2	2.02	30
Li's MENN without system fusion: system 1	6.91	44
Li's MENN without system fusion: system 2	6.64	40
MENN method with system fusion (even λ)	8.11	62
MENN method with system fusion (empirically adjusted λ)	9.36	66
MENN method with system fusion (balanced λ)	10.19	66

Table 1, the higher value of ISNR was obtained from the proposed fusion algorithm, in which the resolution-to-noise balance was optimized using the method developed in Section 3. The number of iterations characterizes the computational complexity of the corresponding algorithms. As the use of Li et al.'s modification of a Hopfield-type NN to solve an optimization problem is basically a direct descent approach [22], hence all presented MENN algorithms have the same order of computational complexity comparable with that of the conventional direct descent iterative schemes.

6. Conclusion

In this paper we present a Hopfield-type multistate MENN for image restoration with system fusion as required for remote sensing imagery although it may also be applied to other fields. The developed MENN algorithm utilizes the unified architecture of the Li's NN, but the interconnection strengths and bias inputs are redefined in such a way that enables the NN to perform solution of an aggregate inverse problem of image restoration from the degraded images received of different systems. The new MENN algorithm contains also some design parameters viewed as the regularization degrees of freedom, which with an adequate selection can improve the overall fusion performance. The method was proposed to perform balanced aggregation of the fusing systems' data to realize the image reconstruction with improved spatial resolution and controllable noise level. The improvement was achieved due to the optimal integration of the use of a priori ME model information, calibration data and redundancy in the measurements provided by different systems. The developed MENN algorithm was tested successfully through computer simulation of the restoration of degraded images obtained with two different passive radar sensing systems operating in a noisy environment. The new method exhibited better overall resolution performances than traditional high-resolution regularized least squares inversion technique and existing neural-network-based image

restoration methods that do not accomplish the system fusion or perform conventional decentralized fusion.

Acknowledgements

The authors would like to thank the anonymous reviewers for their constructive criticism, which helped to improve the presentation of this paper.

References

[1] J. Capon, High-resolution frequency-wavenumber spectrum analysis, Proc. IEEE 57 (1969) 1408–1418.
[2] R.N. McDonough, Application of the maximum-likelihood method and maximum entropy method for array processing, in: S. Haykin (Ed.), Nonlinear Methods of Spectral Analysis, Willey, New York, 1984, pp. 181–244.
[3] Yu. P. Pytyev, Linear problems of image restoration and enhancement, in: Mathematical Methods for Earth Resources Investigation from Space, Nauka, Moscow, 1984, pp. 91–122 (in Russian).
[4] S.L. Marple Jr., Digital Spectral Analysis with Applications, Prentice-Hall Inc., Englewood Cliffs, NJ, 1987.
[5] J. Munier, G.L. Delisle, Spatial analysis in passive listening using adaptive techniques, Proc. IEEE 75 (11) (1987) 21–37.
[6] S.E. Falkovich, V.I. Ponomaryov, Yu.V. Shkvarko, Optimal Reception of Space-Time Signals in Channels with Scattering, Radio i sviaz, Moscow, 1989 (in Russian).
[7] E. Waltzs, J. Llinas, Multisensor Data Fusion, Artech House, Boston, 1990.
[8] A. Farina, Antenna-Based Signal Processing Techniques for Radar Systems, Artech House, Boston, 1992.
[9] D.L. Hall, Mathematical Techniques in Multisensor Data Fusion, Artech House, Boston, London, 1992.
[10] B. Kosko, Neural Networks for Signal Processing, Prentice-Hall, New York, 1992.
[11] G.A. Baxes, Digital Image Processing: Principles and Applications, Wiley, New York, 1994.
[12] S. Haykin, Neural Networks: A Comprehensive Foundation, Macmillan, New York, 1994.
[13] R.T. Anthony, Principles of Data Fusion Automation, Artech House, Boston, 1995.
[14] F.M. Henderson, A.V. Lewis (Eds.), Principles and Applications of Imaging Radar, Manual of Remote Sensing, Vol. 3, 3rd Edition, Wiley, New York, 1998.
[15] Y.T. Zhou, R. Chellappa, A. Vaid, B.K. Jenkins, Image restoration using a neural network, IEEE Trans. Acoust. Speech Signal Process. 36 (1988) 38–54.
[16] N.P. Galatsanos, A.K. Katsaggelos, B.T. Chin, A.D. Hillery, Least squares restoration of multichannel images, IEEE Trans. Acoust. Speech Signal Process. 39 (1991) 2222–2236.
[17] D. Ingman, Y. Merlis, Maximum entropy signal reconstruction with neural networks, IEEE Trans. Neural Networks 3 (1992) 195–201.
[18] N.L. Novak, C. Netishen, Polarimetric synthesis aperture radar imaging, Int. J. Imaging System Technol. (1992) 306–318.
[19] J.K. Paik, A.K. Katsaggelos, Image restoration using a modified Hopfield network, IEEE Trans. Image Process. 1 (1992) 49–63.
[20] B. Yoshua, F. Paolo, An EM approach to learning sequential behavior, Technical Report, RT-DSI 11, University of Florence, 1994.
[21] Yu.V. Shkvarko, Yu.V. Kostenko, Combined statistical regularization and experiment design theory-based nonlinear techniques for extended object imaging from remotely sensed data, SPIE International Symposium on Aerospace Sensing, Vol. SPIE 2232, 1994, pp. 309–317.

[22] H.D. Li, M. Kallergi, W. Qian, V.K. Jain, L.P. Clarke, Neural network with maximum entropy constraint for nuclear medicine image restoration, Opt. Eng. 34 (5) (1995) 1431–1440.
[23] L. Han, S.K. Biswas, Neural networks for sinusoidal frequency estimation, J. Franklin Inst. 334B (1) (1997) 1–18.
[24] R.A. Jacobs, P. Fengchun, M.A. Tanner, A Bayesian approach to model selection in hierarchical mixtures-of-experts architectures, Neural Networks 10 (2) (1997) 231–241.
[25] L. Rebollo-Neira, J. Fernandes-Rubio, The continuous wavelet transform as a maximum entropy solution of the corresponding inverse problem, IEEE Trans. Signal Process. 47 (7) (1999) 2046–2050.
[26] K. Harmanci, J. Tabrikian, J.L. Krolik, Relationship between adaptive maximum variance beamforming and optimal source localization, IEEE Trans. Signal Process. 48 (1) (2000) 1–13.